Electronic Supplementary Material (ESI) for Soft Matter.

Supporting Information for:

Insight into Polymerization-Induced Self-Assembly by Dissipative Particle Dynamics Simulation

Feng Huang, Yisheng Lv, Liquan Wang,* Pengxiang Xu, Jiaping Lin and Shaoliang Lin*

1. Variation of internal chains amounts inside the aggregate

Fig. S1 shows variation of internal chains as a function of simulation time. As shown in Figure S1, the amounts of the internal chains increase in the transition of initial stage. This suggests that the transfer of the external chains into the center of micelle could stabilize the structures.

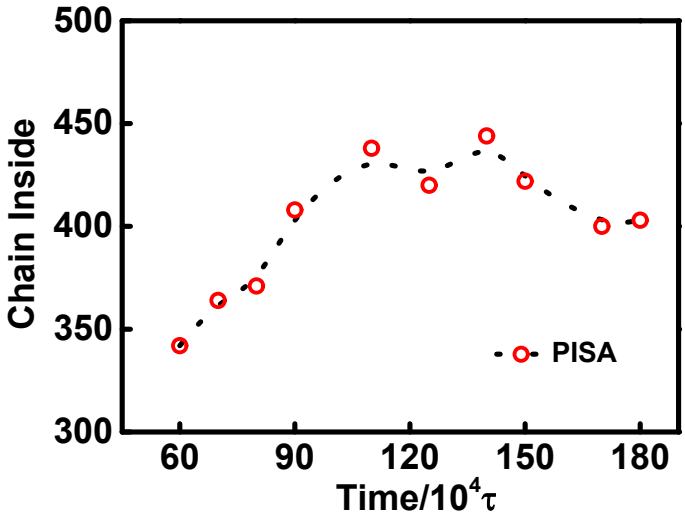

Fig. S1 Variation of internal chains amounts as a function of simulation time, where the morphology is changed from vesicle to LCM during the PISA.

2. Comparison of energy

Fig. S2 shows the energy as a function of the simulation steps for the self-assembly alone and the polymerization-induced self-assembly. As shown in the Figure, the energy of large-compound micelles is less than that of the vesicles formed with polymerization. Therefore, the large-compound micelles formed by self-assembly alone are more stable.

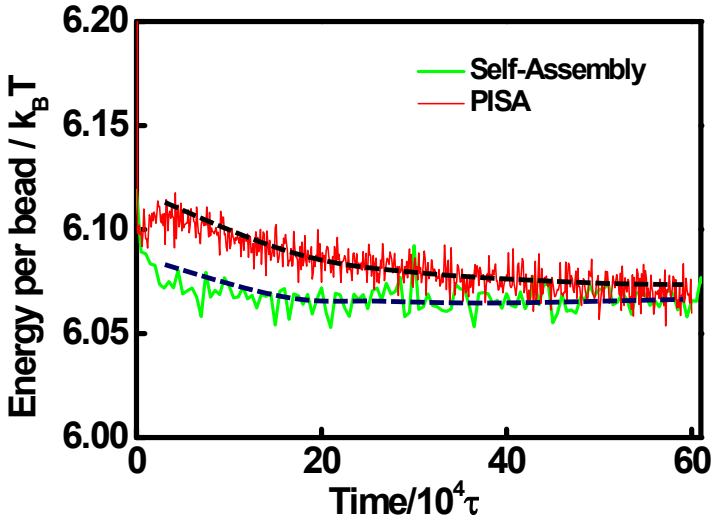

Fig. S2 Plot of energy as a function of the simulation step. The composition of self-assembly alone is the same as that of PISA at $6\times10^5\tau$. The dot lines are drawn to guide eyes.

3. Effect of polymerization rate on the aggregates

Fig. S3 shows representative structures obtained in the PISA with reaction probability P_r=0.01 at various simulation times. As shown in Figure S3, fast polymerization dominates of this initial stage, and it only cost $5\times10^4\tau$ to achieve 100% monomer conversion. Therefore, the following stage is controlled by the self-assembly, and the evolution of the aggregates is the similar to the traditional self-assembly (see Figure 7) with the transition from micelle "diffusion" to form LCMs (see Figure S3b-c).

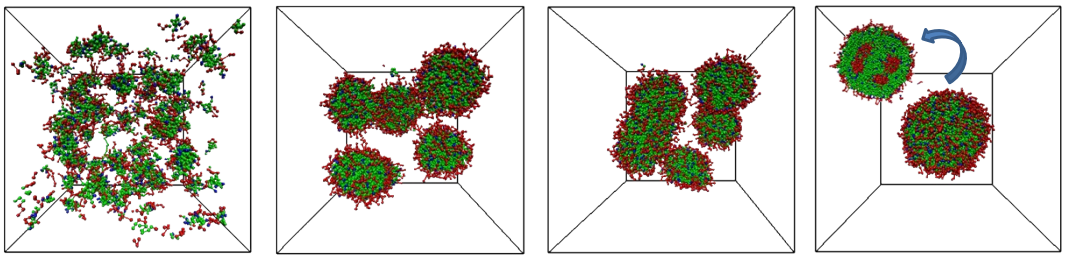

Figure S3. Representative structures obtained in the PISA with reaction probability P_r = 0.01 at various simulation times: (a) $2\times10^3\tau$, (b) $5\times10^4\tau$, (c) $2\times10^5\tau$, and (d) $5\times10^5\tau$.

4. Morphological diagram

Fig. S4 shows the morphology diagram as a functional of total initial concentration of macromolecular initiators and monomers for various targeted DP. It was found that the targeted DP plays a significant impact on the morphologies of the aggregates. At low targeted DP of 2, the polymers with short hydrophobic block are able to form loose aggregates, especially spherical micelles. As the targeted DP is increased to 4, more monomers would be consumed to form hydrophobic blocks. As a result, the spherical micelles coalesce to form wormlike micelle. With further increasing the targeted DP, the morphology changes to vesicle and then arranges to form LCM to minimize the free energy. Note that the total initial concentration of macromolecular initiators and monomers shows less marked influence on the morphologies.

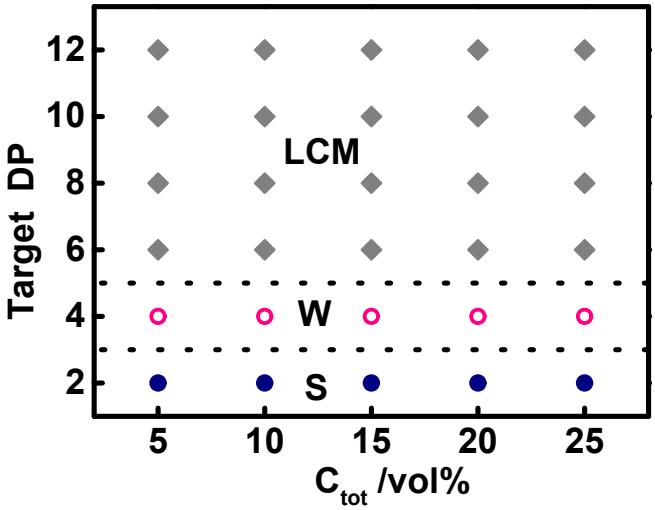

Fig. S4 Morphology stability regions in the space of total solid concentration versus targeted *DP*. The macromolecular initiators are A_3C_1. The letters **S**, **W**, and **LCM** represent spherical micelle, worm-like micelle, and large-compound micelle, respectively.

5. Effect of concentration and polymerization rate on the size of aggregates

Fig. S5 shows the size of the aggregates as function of total initial concentrations for the targeted A_3B_4 and A_3B_8. As shown in the Figure, the size increases as the total initial concentration increases. Moreover, the reaction probability shows less pronounced effect on the size of the aggregates.

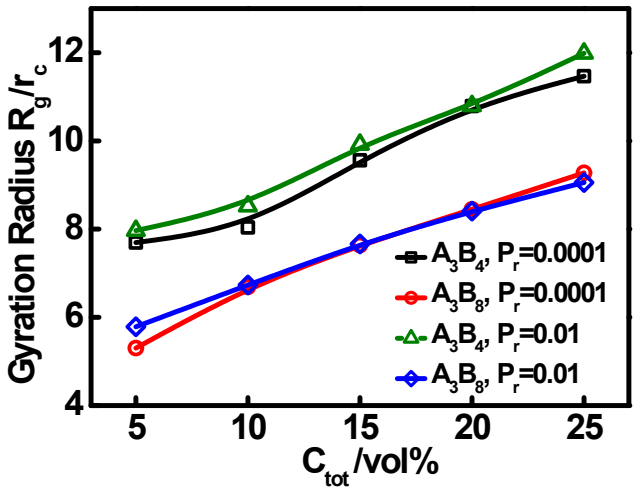

Fig. S5 Variation of gyration radius R_g of the equilibrium aggregates as a function of total initial concentrations C_{tot} of macromolecular initiators and monomers.